Article

Cell Reports

NGL-2 Deletion Leads to Autistic-like Behaviors Responsive to NMDAR Modulation

Graphical Abstract

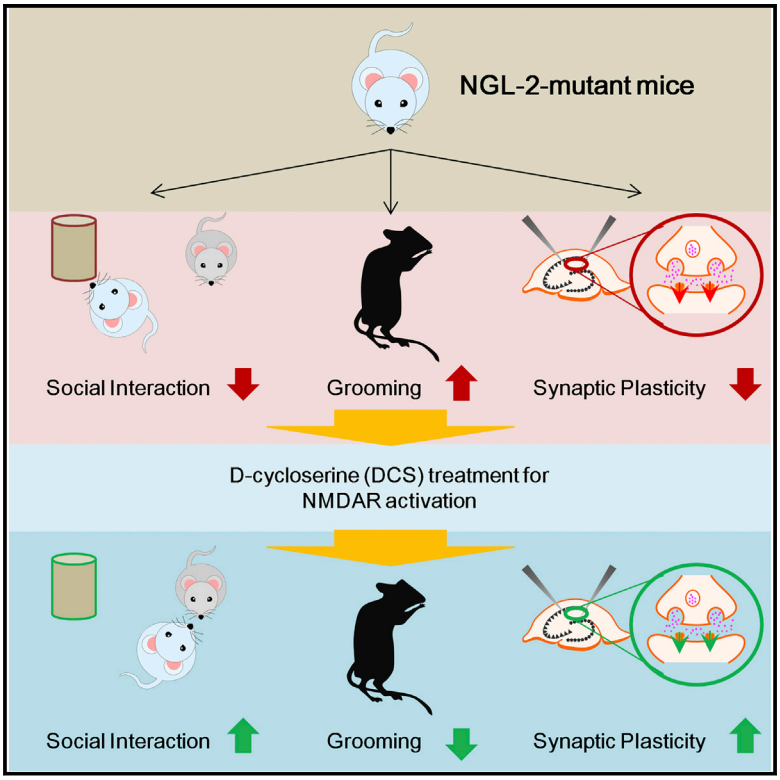

Authors

Seung Min Um, Seungmin Ha, Hyejin Lee, ..., Yeonsoo Choi, Yong Chul Bae, Eunjoon Kim

Correspondence

kime@kaist.ac.kr

In Brief

NGL-2 is a postsynaptic adhesion molecule known to regulate synaptic transmission, but whether NGL-2 regulates synaptic plasticity and specific behaviors remains unknown. Um et al. find that mice lacking NGL-2 display suppressed NMDA receptor-dependent synaptic plasticity and autistic-like social deficits and repetitive behaviors that are responsive to NMDA receptor activation.

Highlights

- NGL-2 associates with and clusters NMDA receptors
- NGL-2 deletion in mice suppresses synaptic NMDAR function
- NGL-2 deletion in mice leads to autistic-like behaviors
- Pharmacological NMDAR activation improves autistic-like behaviors

Um et al., 2018, Cell Reports *23*, 3839–3851
June 26, 2018
https://doi.org/10.1016/j.celrep.2018.05.087

CellPress

Cell Reports
Article

NGL-2 Deletion Leads to Autistic-like Behaviors Responsive to NMDAR Modulation

Seung Min Um,[1] Seungmin Ha,[1] Hyejin Lee,[2] Jihye Kim,[2] Kyungdeok Kim,[1] Wangyong Shin,[1] Yi Sul Cho,[3] Junyeop Daniel Roh,[1] Jaeseung Kang,[2] Taesun Yoo,[1] Young Woo Noh,[1] Yeonsoo Choi,[1] Yong Chul Bae,[3] and Eunjoon Kim[1,2,4,*]

[1]Department of Biological Sciences, Korea Advanced Institute for Science and Technology (KAIST), Daejeon 34141, Korea
[2]Center for Synaptic Brain Dysfunctions, Institute for Basic Science (IBS), Daejeon 34141, Korea
[3]Department of Anatomy and Neurobiology, School of Dentistry, Kyungpook National University, Daegu 700-412, Korea
[4]Lead Contact
*Correspondence: kime@kaist.ac.kr
https://doi.org/10.1016/j.celrep.2018.05.087

SUMMARY

Netrin-G ligand 2 (NGL-2)/LRRC4, implicated in autism spectrum disorders and schizophrenia, is a leucine-rich repeat-containing postsynaptic adhesion molecule that interacts intracellularly with the excitatory postsynaptic scaffolding protein PSD-95 and *trans*-synaptically with the presynaptic adhesion molecule netrin-G2. Functionally, NGL-2 regulates excitatory synapse development and synaptic transmission. However, whether it regulates synaptic plasticity and disease-related specific behaviors is not known. Here, we report that mice lacking NGL-2 (*Lrrc4*$^{-/-}$ mice) show suppressed N-Methyl-D-aspartate receptor (NMDAR)-dependent synaptic plasticity in the hippocampus. NGL-2 associates with NMDARs through both PSD-95-dependent and -independent mechanisms. Moreover, *Lrrc4*$^{-/-}$ mice display mild social interaction deficits and repetitive behaviors that are rapidly improved by pharmacological NMDAR activation. These results suggest that NGL-2 promotes synaptic stabilization of NMDARs, regulates NMDAR-dependent synaptic plasticity, and prevents autistic-like behaviors from developing in mice, supporting the hypothesis that NMDAR dysfunction contributes to autism spectrum disorders.

INTRODUCTION

Synaptic cell adhesion molecules play critical roles in the regulation of synapse development and function (Bemben et al., 2015; de Wit and Ghosh, 2016; Krueger et al., 2012; Missler et al., 2012; Shen and Scheiffele, 2010; Südhof, 2017; Takahashi and Craig, 2013; Um and Ko, 2013; Valnegri et al., 2012; Yuzaki, 2011). Previous studies on synaptic adhesion molecules have identified diverse mechanisms associated with *trans*-synaptic adhesions and synapse development. In addition, a growing body of evidence indicates that synaptic adhesion molecules are also involved in the regulation of synaptic transmission and plasticity.

Synaptic adhesion molecules have also been implicated in diverse psychiatric disorders, including autism spectrum disorders (ASDs) (Bourgeron, 2015; de Wit and Ghosh, 2014; Ko et al., 2015; Krueger et al., 2012; Reissner et al., 2013; Südhof, 2017; Takahashi and Craig, 2013). Although extensive efforts have been made to determine whether dysfunctional synaptic adhesion molecules lead to specific synaptic defects and disease-related behavioral abnormalities, the causal relationship between the observed synaptic defects and behavioral abnormalities in mice has remained largely unclear, except for a few examples (Blundell et al., 2010; Rothwell et al., 2014).

NGL-2 (also known as LRRC4) belongs to the netrin-G ligand (NGL) family of synaptic adhesion molecules, which has three known members: NGL-1/LRRC4C, NGL-2/LRRC4, and NGL-3/LRRC4B (Kim et al., 2006; Lin et al., 2003; Woo et al., 2009b). NGL-2 contains leucine-rich repeats (LRRs) and an immunoglobulin (Ig) domain in the extracellular region, a transmembrane domain, and a cytoplasmic region that terminates in a protein-protein interaction domain (PDZ)-binding motif that binds to PSD-95, an abundant scaffolding protein in the postsynaptic density (PSD) of excitatory synapses. NGL-2 is mainly detected at postsynaptic sites (Matsukawa et al., 2014; Woo et al., 2009a) and *trans*-synaptically interacts with presynaptic netrin-G2/laminet-2 (Kim et al., 2006), a glycosylphosphatidylinositol (GPI)-anchored adhesion molecule highly expressed in specific sets of presynaptic axons (Nakashiba et al., 2002; Yin et al., 2002). NGL-2 also associates with N-Methyl-D-aspartate receptors (NMDARs) in a *cis* manner (Kim et al., 2006). These interactions likely promote excitatory synapse development in specific dendritic segments in an input-specific manner (DeNardo et al., 2012; Nishimura-Akiyoshi et al., 2007).

Previous studies using mice lacking NGL-2 (*Lrrc4*$^{-/-}$ mice) have shown that NGL-2 regulates auditory responses (Zhang et al., 2008); excitatory synapse development and synaptic transmission in the hippocampal Schaffer collateral pathway (DeNardo et al., 2012); presynaptic release onto dentate granule cells (Matsukawa et al., 2014); and neurite growth, synapse formation, signal transmission, and restoration in the retina (Soto et al., 2013, 2018). Despite this progress, whether NGL-2 regulates other aspects of synaptic functions such as synaptic plasticity remains unknown.

In addition, the *NGL-2/LRRC4* gene in humans has been implicated in ASDs, schizophrenia, and intellectual disability. A

whole-genome sequencing analysis has identified a missense mutation in *LRRC4* in an individual with ASD (Jiang et al., 2013). *LRRC4* is located in intron 16 of *SND1*, a gene that has been associated with ASDs by SNP analysis (Holt et al., 2010) and *de novo* mutation analysis (Iossifov et al., 2012), and with schizophrenia by copy number variation analysis (Kirov et al., 2012). Two missense mutations of *LRRC4* have been identified in an exome sequencing study of schizophrenia-related Swedish families (Purcell et al., 2014). More recently, a microdeletion including *LRRC4* has been associated with intellectual disability and autism (Sangu et al., 2017). Moreover, netrin-G2, the presynaptic ligand of NGL-2, is linked to schizophrenia and bipolar disorder (Aoki-Suzuki et al., 2005; Eastwood and Harrison, 2008). However, whether the lack of NGL-2 indeed causes behavioral abnormalities in animal models and, if so, whether they are associated with any synaptic defects remain unknown.

Here, we found that mice lacking the *Lrrc4* gene ($Lrrc4^{-/-}$ mice) show suppressed NMDAR-dependent synaptic plasticity. Mechanistically, NGL-2 associates with NMDARs through PSD-95-dependent and -independent mechanisms. $Lrrc4^{-/-}$ mice display social deficits and repetitive behaviors that are rapidly improved by NMDAR activation.

RESULTS

Generation and Basic Characterization of $Lrrc4^{-/-}$ Mice

To explore *in vivo* functions of NGL-2, we generated transgenic mice that lack exon 1 of the mouse *Lrrc4* gene, which contains the complete coding region of the gene and is the only exon in the gene (Figures S1A and S1B). $Lrrc4^{-/-}$ mice lacked detectable expression of NGL-2 proteins in the brain (Figure S1C) and displayed normal gross morphology of the brain, exemplified by the normal layer structure in the hippocampus (Figure S1D). Immunofluorescence signals for excitatory and inhibitory synaptic markers were also normal in the hippocampus (Figures S1E and S1F). The levels of NGL-2 relatives (NGL-1 and NGL-3), or those of netrin-G2 (a presynaptic binding partner of NGL-2), were not changed in the $Lrrc4^{-/-}$ brain, as revealed by immunoblot analysis (Figure S2A). There were no changes in the total and synaptic levels of PSD-95, CaMKIIα/β, and glutamate receptor subunits (GluN1/2A/2B and GluA1/2) (see also Discussion).

$Lrrc4^{-/-}$ Mice Display Mildly Reduced Social Interaction and Suppressed Social Communication

Because NGL-2 has been shown to be associated with ASDs and schizophrenia, we first tested whether $Lrrc4^{-/-}$ mice display social deficits. $Lrrc4^{-/-}$ mice (3–5 months) showed a mild reduction in social interaction but normal social novelty recognition in the three-chamber test, as compared with wild-type (WT) mice (Figures 1A and 1B).

When ultrasonic vocalizations (USVs) were measured, $Lrrc4^{-/-}$ pups (post-natal day [P] 7–11) separated from their mothers emitted fewer USVs and took longer to emit the first USV call (Figure 1C). Adult male $Lrrc4^{-/-}$ mice emitted fewer USVs when they encountered a stranger female mouse, although the time to emission of the first USV call was not changed (Figure 1D). Pup retrieval by female $Lrrc4^{-/-}$ mice was normal (Figure S3A), suggesting that *Lrrc4* deletion is unlikely to affect the ability to hear USVs. When USV patterns were analyzed, $Lrrc4^{-/-}$ pups and adult mice displayed suppressed levels of harmonic and short calls, respectively (Figures S3B–S3G), types of USVs strongly associated with social communications (Fujita et al., 2008; Malkova et al., 2012; Scattoni et al., 2008; Sugimoto et al., 2011; Wang et al., 2008). Together, these results suggest that $Lrrc4^{-/-}$ mice display mildly reduced social interaction and suppressed USVs.

$Lrrc4^{-/-}$ Mice Display Repetitive Behaviors, Impaired Spatial Learning, and Mild Anxiety-like Behaviors

$Lrrc4^{-/-}$ mice showed other behavioral abnormalities. First, $Lrrc4^{-/-}$ mice displayed increased self-grooming in home cages (Figure 2A), as well as in Laboras cages, where mouse movements were continuously monitored for 48 hr (Figure 2B; Figures S4A–S4D).

In the Morris water maze test, $Lrrc4^{-/-}$ mice performed poorly in learning, probe, and reversal phases, while performing normally in the visible platform test (Figures 2C–2F). In the novel object recognition test, however, $Lrrc4^{-/-}$ mice performed normally (Figure 2G), suggesting that $Lrrc4^{-/-}$ mice display impaired spatial learning but normal recognition memory.

$Lrrc4^{-/-}$ mice also displayed modest anxiety-like behaviors. In the light-dark test, $Lrrc4^{-/-}$ mice less frequently visited and spent less time in the light chamber (Figure 2H). They acted normally in elevated plus-maze and open-field tests (Figures S4E–S4G), but had reduced performance in the rotarod test (Figure S4H).

NGL-2 Regulates Excitatory, but Not Inhibitory, Synapse Density and Function

To see whether NGL-2 regulates synapse density and function, we first examined spontaneous synaptic transmission. Both the frequency and amplitude of miniature excitatory postsynaptic currents (mEPSCs) were reduced in hippocampal CA1 pyramidal neurons in $Lrrc4^{-/-}$ mice (P21–P23; Figure 3A). This differs from the recent finding that $Lrrc4^{-/-}$ CA1 pyramidal neurons display mEPSCs with reduced frequency but normal amplitude (DeNardo et al., 2012). This could be attributable to that the previous study used younger slice preparations (P12–P16), a hypothesis in line with the steadily increasing levels of the NGL-2 protein until ~P21 (Figure S2B). Miniature inhibitory postsynaptic currents (mIPSCs) were normal in these neurons (Figure 3B), suggesting that NGL-2 mainly regulates excitatory synapses.

An electron microscopic (EM) analysis indicated that the density of the PSD apposed to presynaptic axon terminals was reduced in the $Lrrc4^{-/-}$ hippocampus (stratum radiatum; 3 weeks; Figure 3C). In addition, PSD length and thickness were reduced, whereas PSD perforation (a measure of mature excitatory synapses) was not changed. Moreover, spine densities, measured by biocytin injection and Golgi staining, were reduced (Figures 3D and 3E), similar to the previous result from DiI injection (DeNardo et al., 2012).

$Lrrc4^{-/-}$ CA1 pyramidal neurons display normal dendritic complexity, as shown by Sholl analysis (Figure 3F). These results collectively suggest that NGL-2 regulates excitatory synapses, but not inhibitory synapses or dendritic complexity.

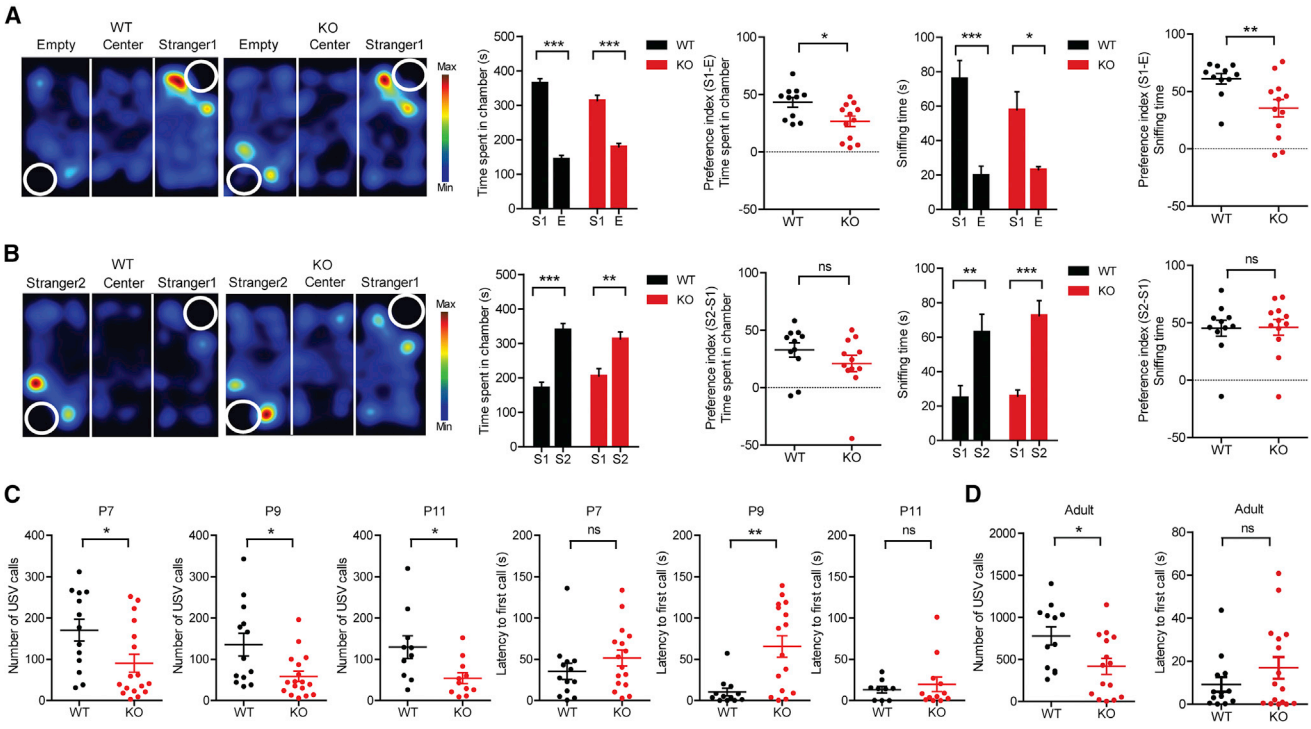

Figure 1. *Lrrc4*$^{-/-}$ Mice Display Mildly Reduced Social Interaction and Suppressed Social Communication

(A and B) Mildly reduced social interaction (A) but normal social novelty recognition (B) in *Lrrc4*$^{-/-}$ mice (3–5 months) in the three-chamber test, as shown by the sniffing time, chamber time, and the preference index ([numerical difference between S1 and O, or S2 and S1]/[sum of S1 and O, S2 and S1] × 100). Data are presented as means ± SEM. n = 11 mice (WT) and 12 (knockout [KO]). *p < 0.05; **p < 0.01; ***p < 0.001; ns, not significant, Student's t test.

(C) Suppressed USV calls in *Lrrc4*$^{-/-}$ pups (P7–P11) separated from their mothers, as shown by USV call number and latency to the first call. n = 14 (WT) and 17 (KO) for P7/P9, and 10 (WT) and 11 (KO) for P11, Student's t test.

(D) Suppressed USV calls in adult male *Lrrc4*$^{-/-}$ mice (2 months) encountering a stranger female mouse. n = 13 (WT) and 15 (KO), Student's t test.

NGL-2 Regulates Excitatory Transmission and NMDAR-Dependent Synaptic Plasticity

Lrrc4 deletion has been shown to suppress evoked excitatory synaptic transmissions mediated by AMPA receptors (AMPARs) and NMDARs (DeNardo et al., 2012). Here, we observed similar decreases in AMPAR- and NMDAR-mediated evoked synaptic transmission at *Lrrc4*$^{-/-}$ Schaffer collateral (SC)-CA1 synapses (P21–P25), as shown by reduced input-output ratios with normal paired-pulse facilitation in field recordings (suggestive of suppressed AMPAR component without a change in presynaptic release) and unchanged ratio of NMDAR- and AMPAR-mediated EPSCs (suppression of both NMDAR and AMPAR components) (Figures 4A–4C). The decay kinetics of NMDAR-EPSCs were not changed (Figure 4D), indicating that both GluN2A and GluN2B subunits are involved. Reduced NMDAR function was also observed in the medial prefrontal cortex and striatum, as shown by NMDAR-mediated mEPSCs (Figures S5A and S5B).

When NMDAR-dependent synaptic plasticity was examined, long-term potentiation (LTP) induced by theta burst stimulation (TBS) was suppressed at *Lrrc4*$^{-/-}$ SC-CA1 synapses at P25–P30 (Figure 4E) and 2–3 months (Figure S5C). Long-term depression (LTD) induced by low-frequency stimulation (LFS) was suppressed (Figure 4F). Metabotropic glutamate receptor (mGluR)-LTD induced by DHPG was suppressed, with the difference becoming evident in the late phase (Figure 4G), which unlikely involves suppressed NMDAR function because hippocampal mGluR-LTD does not require NMDAR activation (Fitzjohn et al., 1999; Huber et al., 2000, 2001). Therefore, *Lrrc4*$^{-/-}$ deletion leads to decreases in NMDAR- and AMPAR-mediated synaptic transmission, NMDAR-dependent synaptic plasticity (LTP and LTD), and mGluR-dependent LTD.

NGL-2 Associates with NMDARs through PSD-95-Dependent and -Independent Mechanisms

NGL-2 may enhance synaptic retention of NMDARs through PSD-95, an abundant postsynaptic scaffolding protein coupled to both NGL-2 and NMDAR subunits (GluN2A and GluN2B) through PDZ interactions. Alternatively, some PSD-95-independent mechanisms might be involved. To this end, we tested whether NGL-2 colocalizes with NMDAR subunits in the presence or absence of PSD-95 in heterologous cells.

Singly expressed NGL-2 or GluN1/2A/2B showed a network-like distribution pattern, likely reflecting localizations to the endoplasmic reticulum and Golgi apparatus (Figure 5A). PSD-95, in contrast, showed a diffuse distribution pattern throughout the cell, including the cell periphery. Doubly expressed NGL-2 and PSD-95 formed discrete clusters, often of a large size, containing both proteins (Figure 5B). When NGL-2, PSD-95, and

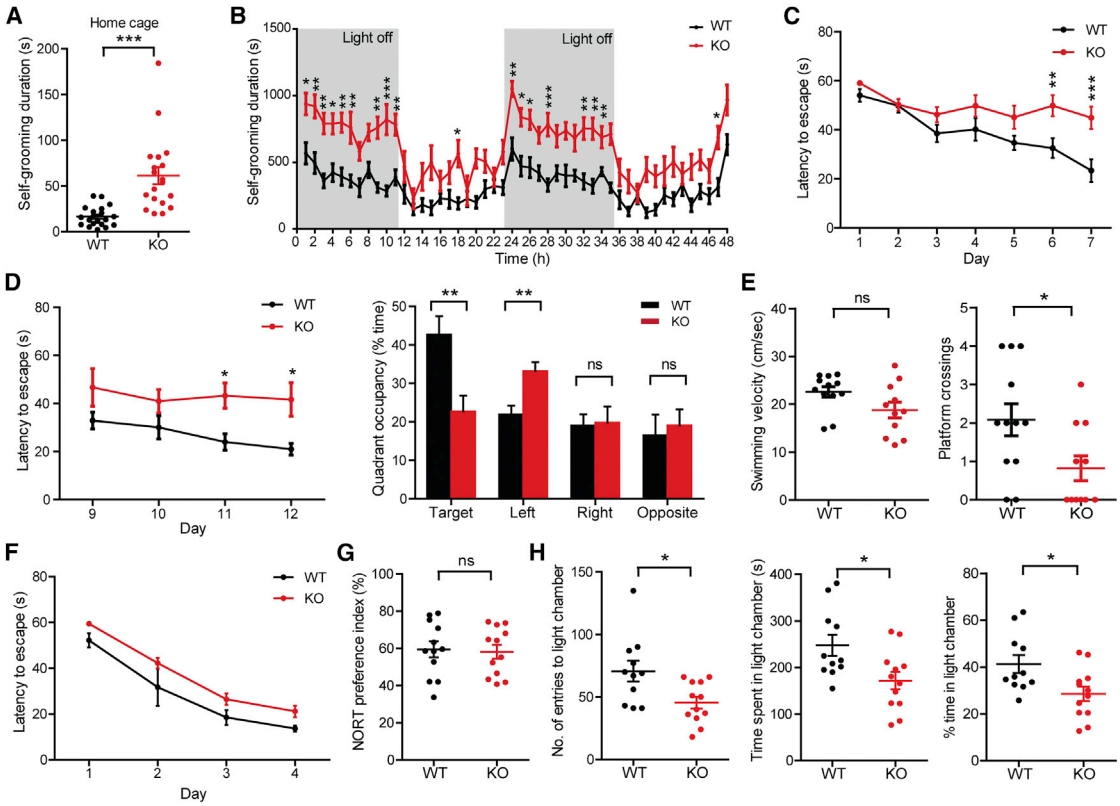

Figure 2. *Lrrc4*$^{-/-}$ Mice Display Repetitive Behaviors, Impaired Spatial Learning, and Mild Anxiety-like Behaviors

(A) Enhanced self-grooming of *Lrrc4*$^{-/-}$ mice (3–5 months) in home cages. Mean ± SEM. n = 20 (WT) and 19 (knockout [KO]) mice, Student's t test.

(B) Enhanced self-grooming of *Lrrc4*$^{-/-}$ mice (3–5 months) in Laboras cages, used for continuous monitoring of diverse movements for 72 hr. n = 12 (WT, KO), two-way ANOVA with Bonferroni test.

(C–E) Reduced spatial learning of *Lrrc4*$^{-/-}$ mice (5 months) in the Morris water maze, as shown by their performances in the learning (C), probe (D), and reversal (E) phases. Quadrant occupancy, platform crossings, and swimming speed were measured during the probe test. n = 12 (WT) and 11 (KO), repeated-measures (RM) two-way ANOVA and Student's t test.

(F) *Lrrc4*$^{-/-}$ mice (5 months) perform normally in the visible platform version of the Morris water maze, as shown by escape latency. n = 5 (WT) and 9 (KO), RM two-way ANOVA.

(G) Normal recognition memory by *Lrrc4*$^{-/-}$ mice (3 months) in the novel object recognition test, as shown by the preference of the subject mouse for a novel object. n = 12 (WT) and 11 (KO), Student's t test.

(H) Enhanced anxiety-like behavior (3 months) in the light-dark test, as shown by the number of entries into the light chamber, time spent in light chamber, and percentage of time spent in light chamber. n = 11 (WT) and 12 (KO), Student's t test.

*p < 0.05; **p < 0.01; ***p < 0.001; ns, not significant.

GluN1/2A/2B were triply coexpressed, all three proteins were colocalized in discrete clusters (Figure 5C).

Given that GluN1 does not contain a C-terminal PDZ-binding motif, GluN1 likely associates with NGL-2 through PSD-95-independent mechanisms. Indeed, GluN1 coexpressed with PSD-95 in the absence of NGL-2 failed to form discrete clusters (Figure 5D). GluN2A and GluN2B, however, have the C-terminal PDZ-binding motif and may directly associate with PSD-95, in addition to the indirect interactions through NGL-2. To clarify this, we generated mutant forms of GluN2A and GluN2B that lack the C-terminal PDZ-binding motif (GluN2AΔC and GluN2BΔC; deletion of the last 3 aa residues), and thus cannot cocluster with PSD-95 (Figure 5D). However, when GluN2AΔC or GluN2BΔC was triply coexpressed with NGL-2 and PSD-95, GluN2AΔC or GluN2BΔC could still colocalize with NGL-2- and PSD-95-containing clusters (Figure 5E). These results collectively suggest that NGL-2 associates with NMDAR subunits through both PSD-95-dependent and -independent mechanisms.

NMDAR Activation Normalizes Social Interaction and Self-Grooming in *Lrrc4*$^{-/-}$ Mice

Because *Lrrc4*$^{-/-}$ mice display social and repetitive behavioral deficits that are associated with reduced NMDAR function, we reasoned that normalizing the suppressed NMDAR function might rescue the abnormal behaviors. Treatment of *Lrrc4*$^{-/-}$ mice (3–5 months) with the NMDAR agonist D-cycloserine (DCS; 20 mg/kg; intraperitoneal [i.p.]) 20 minutes before the three-chamber test improved social interaction, as shown by sniffing (but not chamber) time and the preference index (Figures 6A–6C). DCS minimally affected social interaction in WT mice. In additional three-chamber tests with a modified protocol to rule out directional bias (Bidinosti et al., 2016; Duffney et al., 2015;

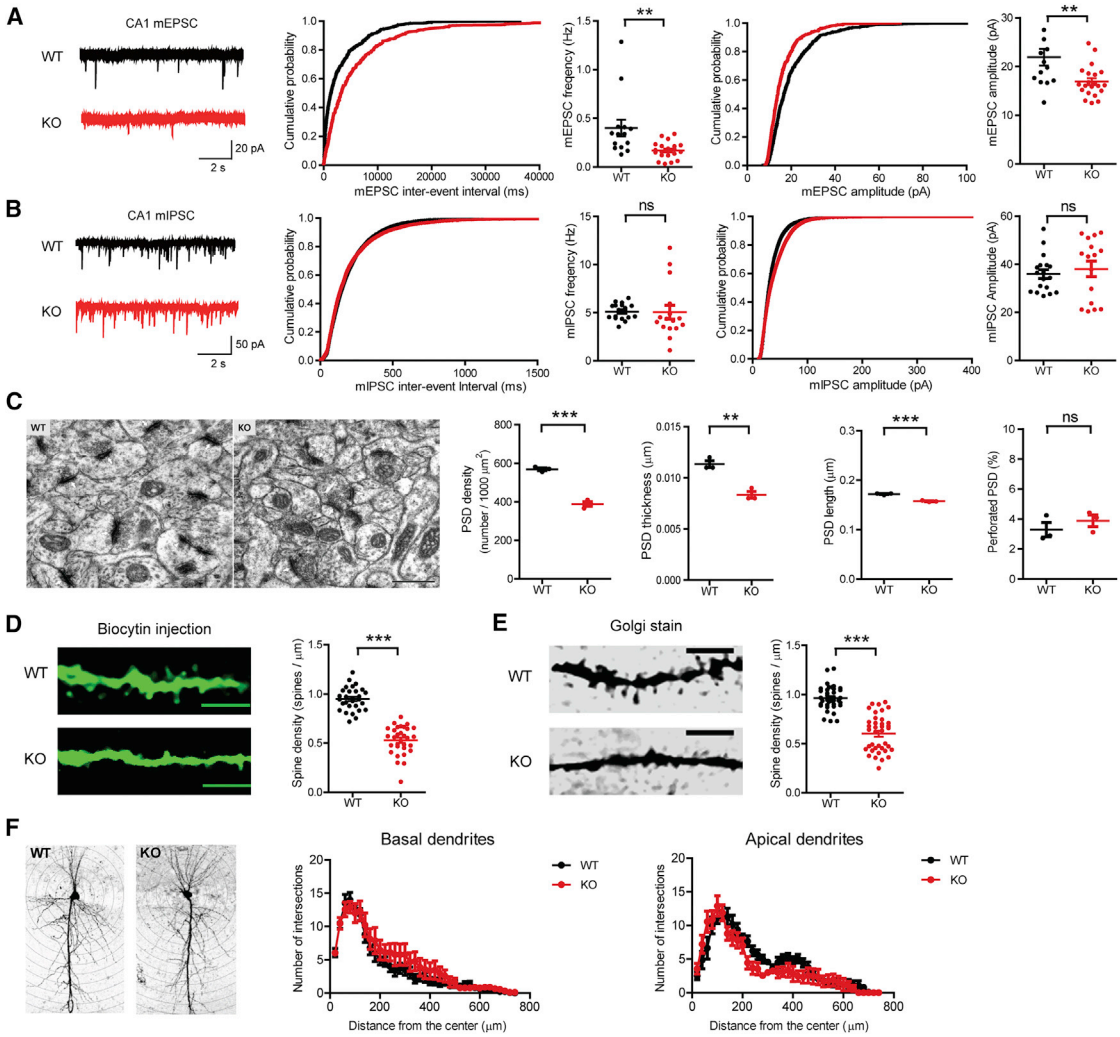

Figure 3. *Lrrc4* Deletion Suppresses Excitatory, but Not Inhibitory, Synapse Density and Function in the Hippocampus

(A) Reduced frequency and amplitude of mEPSCs in *Lrrc4*$^{-/-}$ CA1 pyramidal neurons (P21–P23). Mean ± SEM. n = 18 neurons from 6 mice (WT) and n = 19 neurons from 7 mice (knockout [KO]), Student's t test.

(B) Normal frequency and amplitude of mIPSCs in *Lrrc4*$^{-/-}$ CA1 pyramidal neurons (P21–P23). n = 18 neurons from 4 mice (WT) and n = 16 neurons from 4 (KO) mice, Student's t test.

(C) Reduced density, length, and thickness, but normal perforation, of the PSD in the CA1 stratum radiatum region of the *Lrrc4*$^{-/-}$ hippocampus (P21), as determined by EM analysis. Arrows indicate PSDs, and arrowheads indicate perforated PSDs. n = 3 mice (WT, KO), Student's t test. Scale bar, 500 nm.

(D) Reduced spine density in the *Lrrc4*$^{-/-}$ CA1 stratum radiatum (P20–P23), as determined by biocytin injection. n = 29 dendritic segments from 4 mice (WT) and n = 31 dendritic segments from 4 mice (KO), Student's t test. Scale bars, 5 μm.

(E) Reduced spine density in the *Lrrc4*$^{-/-}$ CA1 stratum radiatum (2–3 months), as determined by Golgi staining. n = 37 dendritic segments from 4 mice (WT) and n = 38 dendritic segments from 4 mice (KO). Scale bars, 5 μm.

(F) Normal complexity of apical and basal dendrites of *Lrrc4*$^{-/-}$ CA1 pyramidal neurons (P21–P24), as determined by Sholl analysis. n = 14 neurons from 3 mice (WT) and n = 9 neurons from 3 mice (KO), two-way ANOVA.

*p < 0.05; **p < 0.01; ***p < 0.001; ns, not significant.

Wang et al., 2011), where mice were exposed to two identical objects before the first social encounter, *Lrrc4*$^{-/-}$ mice did not display directional bias, while showing the same DCS-sensitive social deficits (Figures S6A–S6C). DCS also rapidly improved repetitive self-grooming in *Lrrc4*$^{-/-}$ mice, without affecting WT mice (Figure 6D), but failed to rescue female-induced USVs (Figure 6E), anxiety-like behavior in the light-dark test (Figure 6F), or spatial learning in the Morris water maze test (Figure S6D).

In control experiments, a low-dose DCS (2 mg/kg) failed to rescue social interaction or self-grooming in *Lrrc4*$^{-/-}$ mice (Figures S7A and S7B). The above-mentioned rapid rescue effects of DCS (20 mg/kg) on social interaction and self-grooming were transient, as shown by lack of the rescue effects 24 hr after the DCS treatment (Figures S7C and S7D). In addition, chronic treatment of DCS over 7 days (once a day; 20 mg/kg) did not rescue social interaction or self-grooming when these behaviors were

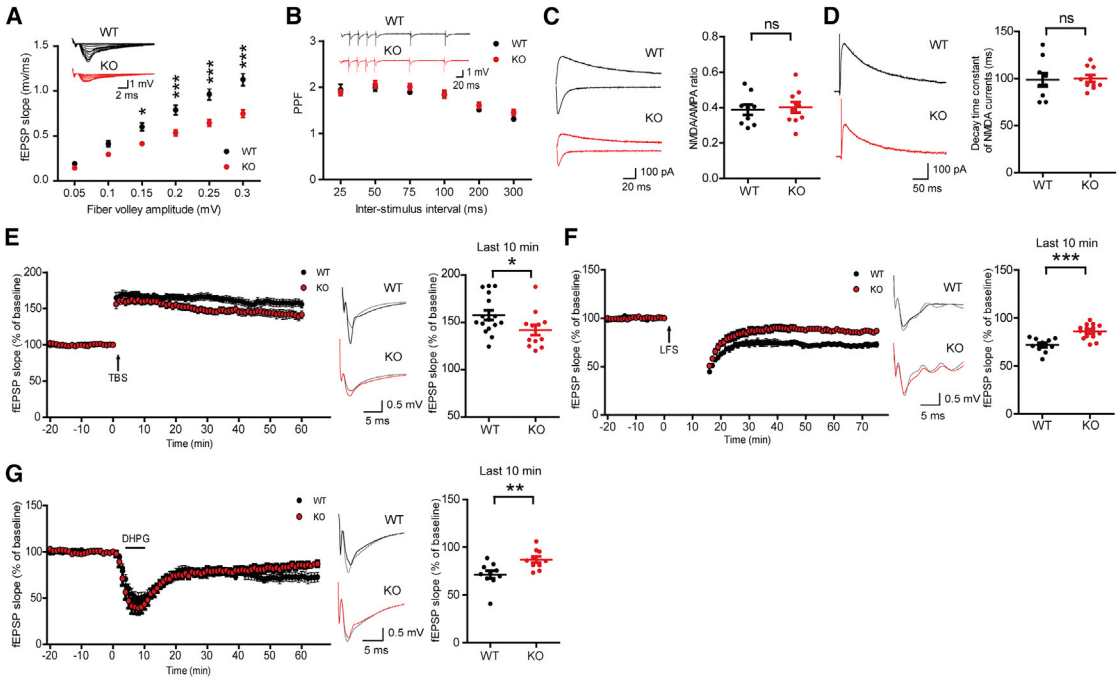

Figure 4. *Lrrc4* Deletion Suppresses Excitatory Transmission and NMDAR- and mGluR-Dependent Synaptic Plasticity

(A) Suppressed excitatory basal transmission at *Lrrc4*$^{-/-}$ SC-CA1 synapses (P21–P25), as shown by field excitatory postsynaptic potential (fEPSP) slopes plotted against fiber volley amplitudes (input-output). Mean ± SEM. n = 9 slices from 3 mice (WT, knockout [KO]), Student's t test.

(B) Normal paired-pulse facilitation at *Lrrc4*$^{-/-}$ SC-CA1 synapses (P21–P25), as shown by fEPSP slopes plotted against inter-stimulus intervals. n = 9 slices from 3 mice (WT, KO), Student's t test.

(C) Unaltered ratio of NMDAR- and AMPAR-EPSCs at *Lrrc4*$^{-/-}$ SC-CA1 synapses (P17–P22). n = 9 neurons from 6 mice (WT) and n = 10 from 7 mice (KO), Student's t test.

(D) Normal decay kinetics of NMDAR-EPSCs at *Lrrc4*$^{-/-}$ SC-CA1 synapses (P17–P22), as determined by analyzing the results in (C).

(E) Suppressed TBS-LTP at *Lrrc4*$^{-/-}$ SC-CA1 synapses (P25–P30). n = 16 slices from 6 mice (WT) and n = 12 slices from 7 mice (KO), Student's t test.

(F) Suppressed LFS-LTD (1 Hz, 900 pulses) at *Lrrc4*$^{-/-}$ SC-CA1 synapses (P17–P22). n = 10 slices from 7 mice (WT) and n = 14 slices from 7 mice (KO), Student's t test.

(G) Suppressed mGluR-LTD induced DHPG at *Lrrc4*$^{-/-}$ SC-CA1 synapses (P21–P25). n = 10 slices from 5 mice (WT, KO), Student's t test.

*p < 0.05; **p < 0.01; ***p < 0.001; ns, not significant.

measured 24–48 hr after the last day of the chronic treatment (Figures S7E and S7F). Lastly, DCS did not affect locomotor activities of WT mice in the open-field test (Figure S6E), suggesting that the DCS-dependent behavioral rescues in *Lrrc4*$^{-/-}$ mice unlikely involve enhanced locomotion.

DCS Restores NMDAR-Dependent Synaptic Transmission and Plasticity in *Lrrc4*$^{-/-}$ Mice

Finally, we tested whether the DCS-dependent social rescue in *Lrrc4*$^{-/-}$ mice involves restoration of NMDAR function. DCS normalized TBS-LTP at *Lrrc4*$^{-/-}$ SC-CA1 synapses (3–4 weeks), without affecting TBS-LTP at WT synapses (Figure 7A). In addition, DCS restored LFS-LTD at *Lrrc4*$^{-/-}$ SC-CA1 synapses (2–3 weeks), without affecting WT synapses (Figure 7B).

To measure NMDAR function more directly, we pharmacologically isolated NMDAR fEPSPs (field excitatory postsynaptic potentials) by 2,3-dihydroxy-6-nitro-7-sulphamoyl-benzo(F)quinoxaline (NBQX) (an AMPAR blocker) under a low-magnesium condition. *Lrrc4*$^{-/-}$ SC-CA1 synapses (P19–P22) displayed decreased slopes and peaks of NMDAR fEPSPs, and DCS normalized these parameters, without affecting WT synapses (Figure 7C). These results collectively suggest that DCS restores NMDAR-dependent synaptic transmission and plasticity in *Lrrc4*$^{-/-}$ mice.

DISCUSSION

Our data implicate NGL-2 in the regulation of excitatory synaptic transmission and plasticity. NMDAR- and AMPAR-mediated synaptic transmission at SC-CA1 synapses has been shown to be suppressed by *in utero Lrrc4* knockdown and *in vivo Lrrc4* knockout (DeNardo et al., 2012). Our study confirms these results and extends them by showing that *Lrrc4* deletion leads to decreases in NMDAR-dependent HFS-LTP and LFS-LTD and mGluR-LTD at SC-CA1 synapses. In addition, many synaptic adhesion molecules, including neuroligins, neurexins, and EphB, regulate synaptic transmission and plasticity (Jang et al., 2017). Our findings add NGL-2 to this list as a postsynaptic adhesion molecule that regulates NMDAR-dependent synaptic transmission and plasticity.

The reduced NMDAR function in the *Lrrc4*$^{-/-}$ hippocampus does not match with the normal levels of total and synaptic

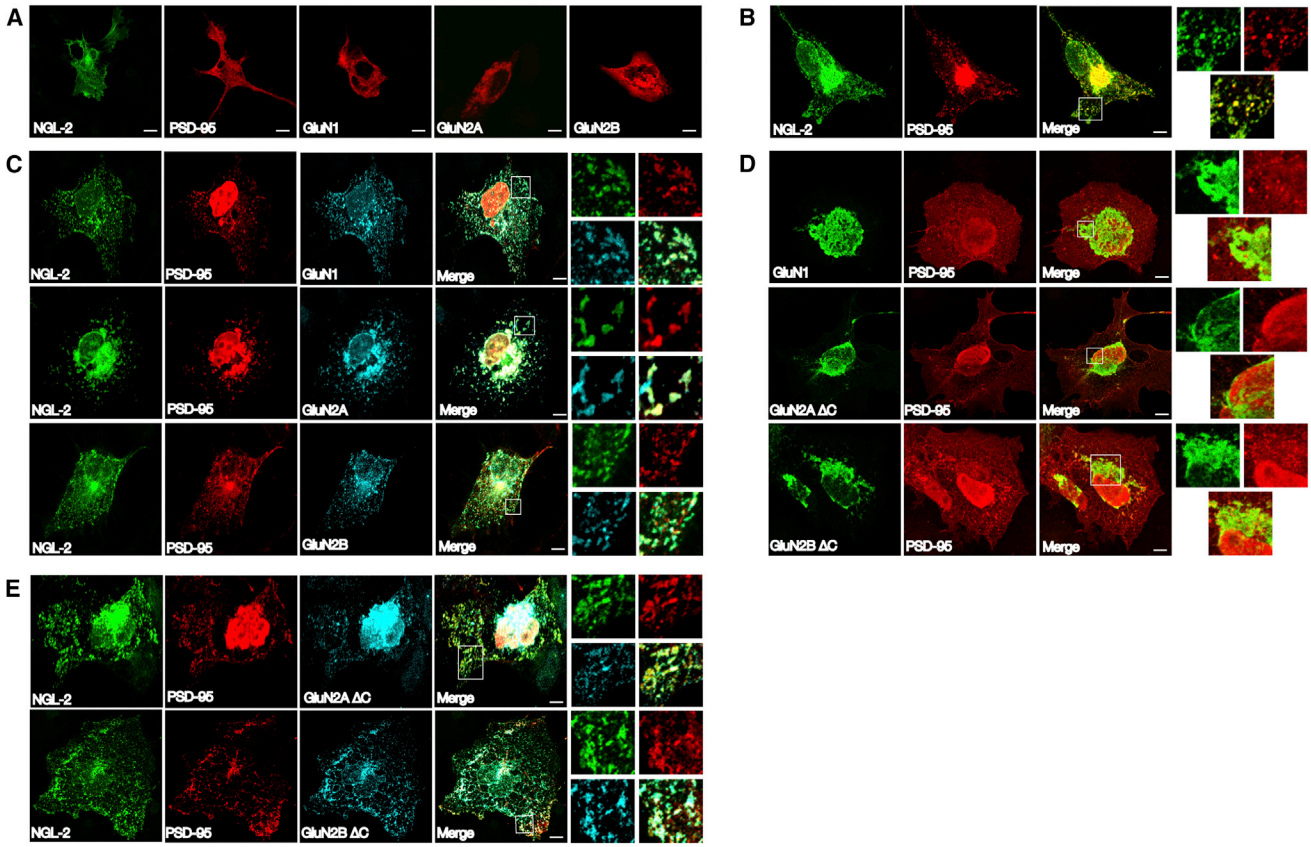

Figure 5. NGL-2 Associates with NMDARs through PSD-95-Dependent and -Independent Mechanisms

(A) NGL-2 (Myc-NGL-2), PSD-95 (HA-PSD-95), or GluN1/2A/2B proteins (untagged) singly expressed in COS-7 cells show largely perinuclear or widespread distribution patterns. Scale bars, 10 μm.

(B) NGL-2 and PSD-95 doubly expressed in COS-7 cells colocalize in discrete clusters. Scale bar, 5 μm.

(C) NGL-2, PSD-95, and NMDAR subunits (GluN1, GluN2A, and GluN2B) triply expressed in COS-7 cells colocalize in discrete clusters. Scale bars, 10 μm.

(D) GluN1 or mutant GluN2B subunits (GluN2AΔC and GluN2BΔC) doubly expressed with PSD-95 in COS-7 cells in the absence of NGL-2 show largely non-overlapping distribution patterns. Scale bars, 5 μm (GluN1/2B); 10 μm (GluN2A).

(E) Mutant GluN2 subunits (GluN2AΔC and GluN2BΔC) triply expressed in COS-7 together with NGL-2 and PSD-95 still colocalize with other proteins in discrete clusters. Scale bars, 10 μm.

NMDAR subunits determined by immunoblot analysis. A possible explanation is that synaptic NMDAR function can be regulated by posttranslational modifications in addition to synaptic levels (Lussier et al., 2015). In addition, postsynaptic NGL-2 and NGL-1 *trans*-synaptically interact with their presynaptic ligands netrin-G1 and netrin-G2, respectively, promoting the development of largely non-overlapping neuronal pathways (Kim et al., 2006; Lin et al., 2003; Nakashiba et al., 2000, 2002; Nishimura-Akiyoshi et al., 2007; Yin et al., 2002). Lastly, NGL-2/LRRC4 is expressed in glial cells in addition to neurons and modulates glial development and tumorigenesis (Li et al., 2014).

How might NGL-2 regulate synaptic NMDAR function? NGL-2 forms a complex with NMDARs in the rat brain, and bead-induced primary clustering of NGL-2 induces secondary clustering of NMDARs, but not AMPARs (Kim et al., 2006). Here, we found that NGL-2 associates with NMDAR subunits through PSD-95-dependent and -independent mechanisms. PSD-95, which interacts with both NGL-2 and NMDARs, may bring them closer to each other, promoting the formation of a ternary complex and the stabilization of synaptic NMDARs. However, given the known abundance of NMDARs in the brain revealed by proteomics studies (Cheng et al., 2006; Peng et al., 2004), synaptic NMDARs may outnumber NGL-2, and NGL-2 may merely represent one of many mechanisms that promote synaptic NMDAR stabilization. This might be the reason why NMDAR functions were not completely abolished in the *Lrrc4*$^{-/-}$ hippocampus.

Social deficits and repetitive behaviors observed in *Lrrc4*$^{-/-}$ mice represent two core autistic-like behaviors. Dual deficits in social and repetitive behaviors have been observed in only a handful of mouse lines lacking ASD-related synaptic adhesion molecules including neuroligins (Blundell et al., 2010; Etherton et al., 2009, 2011; Radyushkin et al., 2009; Rothwell et al., 2014; Tabuchi et al., 2007; also see Chadman et al., 2008), neurexins (Born et al., 2015; Dachtler et al., 2014; Rabaneda et al., 2014), and MDGA2 (Connor et al., 2016).

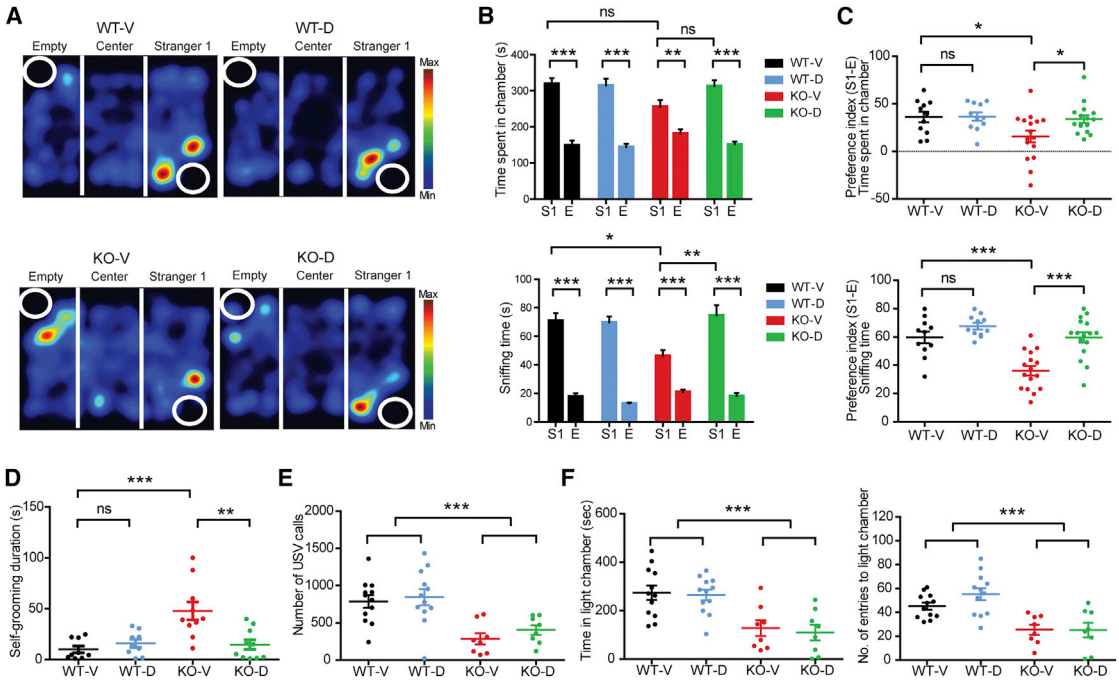

Figure 6. NMDAR Activation by DCS Normalizes Social Interaction and Self-Grooming but Has No Effect on USVs or Anxiety-like Behavior in *Lrrc4*$^{-/-}$ Mice

(A–C) DCS rescues the reduced social interaction of *Lrrc4*$^{-/-}$ mice (3–5 months) in the three-chamber test, as shown by representative heatmaps (A), the time spent in the chamber and sniffing the target (B), and social preference indices derived from these parameters (C). Mean ± SEM. n = 11 (WT-vehicle/V), 11 (WT-DCS/D), 16 (knockout [KO]-V), and 16 (KO-D) mice, Student's t test (S1-E comparison), two-way ANOVA with Holm-Sidak test (S1 and index comparisons).

(D) DCS rescues enhanced self-grooming in *Lrrc4*$^{-/-}$ mice (3–5 months). n = 9 mice (WT-V, WT-D), n = 10 (KO-V, KO-D), two-way ANOVA with Holm-Sidak test.

(E) DCS has no effect on the USV calls emitted by *Lrrc4*$^{-/-}$ mice (4–5 months) upon female encounters, as shown by number of USV calls. n = 12 mice (WT-V, WT-D), n = 8 mice (KO-V, KO-D), two-way ANOVA with Holm-Sidak test ($p = 0.7535$ [interaction], $p = 0.3562$ [drug], and $p < 0.001$ [gene]).

(F) DCS has no effect on the anxiety-like behaviors of *Lrrc4*$^{-/-}$ mice (4–5 months) in the light-dark test, as shown by time in light chamber and number of entries to light chamber. n = 12 mice (WT-V, WT-D), n = 8 (KO-V, KO-D), two-way ANOVA with Holm-Sidak test ($p = 0.8945$ [interaction], $p = 0.6481$ [drug], and $p < 0.001$ [gene]; $p = 0.275$ [interaction], $p = 0.3104$ [drug], and $p < 0.001$ [gene]).

*$p < 0.05$; **$p < 0.01$; ***$p < 0.001$; ns, not significant.

It should be pointed out that *Lrrc4*$^{-/-}$ mice show mild social deficits in the three-chamber test (Figure 1A). This was particularly evident when the social interaction was judged chamber time, as compared with sniffing time or the social preference index. It is possible that *Lrrc4* deletion in mice may have stronger influences on close social interactions such as sniffing than on more indirect social interactions such as staying in the same chamber.

Reduced NMDAR function has been associated with autistic-like behaviors in animal models of ASD (Blundell et al., 2010; Bozdagi et al., 2013; Burket et al., 2013, 2015a, 2015b; Duffney et al., 2013, 2015; Huang et al., 2014; Jacobs and Tsien, 2017; Jaramillo et al., 2016; Kouser et al., 2013; Lee et al., 2015a, 2015b; Qin et al., 2018; Won et al., 2012). Our results further support this emerging notion.

Moreover, NMDAR activation in mice lacking Shank2, Tbr1, and neuroligin-1 have been shown to rescue either social interaction or repetitive behaviors (Blundell et al., 2010; Huang et al., 2014; Won et al., 2012), but not both types of behaviors as in *Lrrc4*$^{-/-}$ mice. Our study is the first case of such dual rescues to the best of our knowledge, although DCS-dependent dual rescues of social and repetitive behaviors have been reported in non-transgenic animals such as BALB/c and BTBR mice (Burket et al., 2013; Deutsch et al., 2012). More importantly, our results suggest that the social deficits and repetitive behaviors observed in *Lrrc4*$^{-/-}$ mice may share the same synaptic pathophysiology while the underlying neural circuits might be different.

DCS did not affect the sociability of WT mice in our study, contrary to the reported prosocial effects of DCS on WT mice (Burket et al., 2013; Deutsch et al., 2011, 2012; Jacome et al., 2011; McAllister, 1994). However, these studies used concentrations of DCS (32–320 mg/kg) that are higher than that used in the present study (20 mg/kg); this low concentration also had no effect on the sociability of WT mice in another study using *Tbr1*-haploinsufficient mice (Huang et al., 2014). Alternatively, differences in mouse strains may provide an explanation; i.e., BALB/c mice display weaker sociability relative to the C57BL/6J strain used in the present study (Brodkin et al., 2004; Deutsch et al., 2011, 2012; Jacome et al., 2011; Sankoorikal et al., 2006), suggesting that WT C57BL/6J mice might have a higher threshold for DCS-dependent prosocial effects.

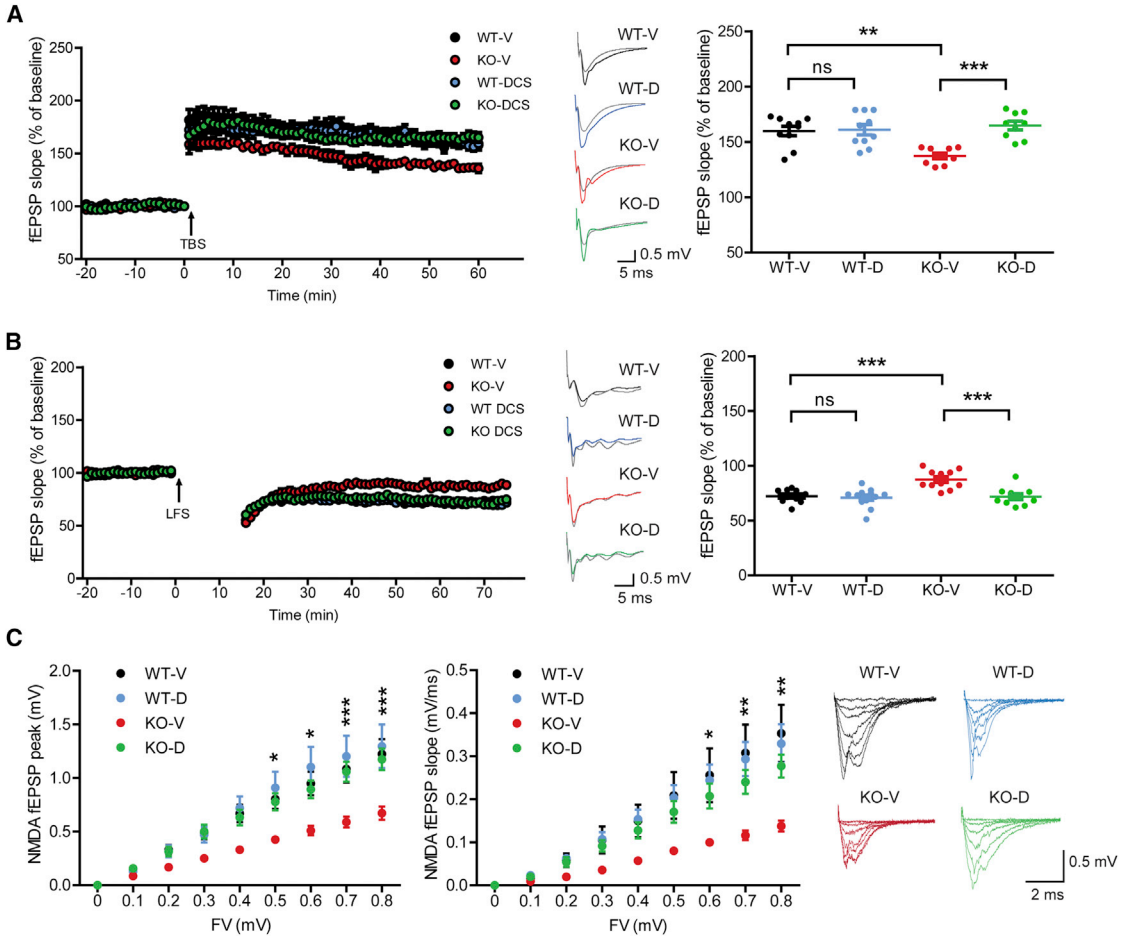

Figure 7. DCS Restores NMDAR-Dependent Synaptic Transmission and Plasticity in the *Lrrc4*$^{-/-}$ Hippocampus

(A) DCS (20 μM) restores suppressed TBS-LTP at *Lrrc4*$^{-/-}$ SC-CA1 synapses (3–4 weeks). Mean ± SEM. n = 10 slices from 6 mice (WT-vehicle/V), n = 9 slices from 7 mice (WT-DCS/D), n = 10 slices from 7 mice (KO-V), and n = 9 slices from 6 mice (KO-D), two-way ANOVA with Holm-Sidak test.

(B) DCS (20 μM) restores LFS-LTD at *Lrrc4*$^{-/-}$ SC-CA1 synapses (2–3 weeks). n = 10 slices from 7 mice (WT-V), n = 11 slices from 7 mice (WT-D), n = 12 slices from 7 mice (KO-V), and n = 10 slices from 7 mice (KO-D), two-way ANOVA with Holm-Sidak test.

(C) DCS (20 μM) restores suppressed NMDAR function at *Lrrc4*$^{-/-}$ SC-CA1 synapses (P19–P22), as shown by fEPSP peaks and slopes plotted against fiber volley amplitudes. n = 11 slices from 4 mice (WT-V), n = 11 slices from 4 mice (WT-D), n = 13 slices from 4 mice (KO-V), and n = 11 slices from 4 mice (KO-D), two-way ANOVA with Bonferroni test (statistical differences between KO-V and KO-D are indicated).

**p < 0.01; ***p < 0.001; ns, not significant.

In addition to prosocial effects, DCS can enhance locomotor activities (Burket et al., 2013; Deutsch et al., 2011, 2012) and memory consolidation in the elevated plus-maze (Rodgers et al., 2011). These mechanisms unlikely underlie our rescue results because DCS does not affect open-field locomotion of WT mice and does not improve anxiety-like behaviors or spatial memory in *Lrrc4*$^{-/-}$ mice (Figures 6F and S6). However, one of the two rescued behaviors (social interaction and repetitive behavior) might still represent an indirect consequence of the other rescue, considering that the concentration of DCS used in the present study (20 mg/kg) is still higher than those used for human individuals with ASDs (i.e., 0.7–2.8 mg/kg) (Posey et al., 2004; Urbano et al., 2014), although rodents generally have higher metabolic rates.

DCS does not rescue USVs or anxiety phenotypes in *Lrrc4*$^{-/-}$ mice, suggesting that these phenotypes may not involve altered NMDAR function. USVs can be regulated by dopamine, noradrenaline, serotonin, GABA, and oxytocin (Rippberger et al., 2015; Scattoni et al., 2009). In addition, anxiety in humans and mice involves diverse mechanisms, including glutamate (NMDAR, AMPAR, mGluR), GABA, serotonin, neuropeptides, and endocannabinoids (Griebel and Holmes, 2013). These non-NMDA mechanisms might underlie the altered USVs and anxiety-like behaviors in *Lrrc4*$^{-/-}$ mice. The lack of DCS-dependent rescue of spatial learning and memory in *Lrrc4*$^{-/-}$ mice might be attributable to that DCS, which has a short half-life (~30 min) (Conzelman and Jones, 1956), may act only during the learning session of the Morris water maze without a long action.

Lrrc4$^{-/-}$ mice may also represent a mouse model of schizophrenia. In support of this possibility, *Lrrc4*$^{-/-}$ mice show reduced social interaction and cognitive impairments, schizophrenia-like

cognitive impairments in rodents (Young et al., 2009), as well as reduced NMDAR function, well-known to be associated with schizophrenia (Jentsch and Roth, 1999; Mohn et al., 1999; Olney et al., 1999), although additional pharmaco-behavioral analyses may be needed.

In conclusion, our data suggest that NGL-2 promotes synaptic stabilization of NMDARs, regulates NMDAR-dependent synaptic plasticity, and regulates social and repetitive behaviors in mice, supporting the emerging hypothesis that NMDAR dysfunction contributes to ASDs.

EXPERIMENTAL PROCEDURES

Additional details are described in the Supplemental Experimental Procedures.

Mouse Generation

We received *Lrrc4*$^{-/-}$ mice from Mutant Mouse Resource and Research Center (MMRRC) (032443_UCD), which were generated using the 129S5/SvEvBrd-derived embryonic stem cell. The whole single exon was targeted by homologous recombination using the β-geo (lacZ/neo) cassette. The chimeric mice were crossed with C57BL/6-Tyrc-Brd albino mice to generate F1 generation, followed by backcrossing with C57BL/6N. *Lrrc4*$^{-/-}$ mice received from MMRRC were crossed with C57BL/6J for more than five generations to perform experiments. These mice were maintained according to the Requirements of Animal Research at KAIST, and experimental procedures were approved by the Committee on Animal Research at Korea Advanced Institute for Science and Technology (KAIST; KA2012-19). Information on mouse sex and ages are as follows: immunoblot analysis (male; P21–22), Golgi staining (male; 2–3 months), Sholl analysis (male; P21–P24), immunohistochemistry (male; P28), electrophysiology (males and females; P14–P30 except for adult LTP [2–3 months]), and behaviors (males; 2–5 months except for pup USV [P7–P11]).

Acute Slice Electrophysiology

Sagittal hippocampal slices (300 μm) from mice (2–4 weeks) anesthetized by isoflurane were prepared using a Vibratome (Leica VT1200) and ice-cold sucrose-based artificial cerebrospinal fluid (aCSF) buffer containing (in mM) 212 sucrose,10 D-glucose, 25 $NaHCO_3$, 5 KCl, 1.25 NaH_2PO_4, 1.25 L-ascorbic acid, 2 Na-pyruvate, 3.5 $MgSO_4$, and 0.5 $CaCl_2$ bubbled with 95% O_2 and 5% CO_2. Brain slices were recovered in a chamber while submerged in aCSF (32°C) containing (mM) 124 NaCl, 10 D-glucose, 25 $NaHCO_3$, 2.5 KCl, 1 NaH_2PO_4, 1.3 $MgCl_2$, and 2.5 $CaCl_2$ for 30 min, and recovered further at room temperature for at least over 30 min.

Drug Rescue

DCS (Sigma) was dissolved in saline, and mice were injected with DCS (20 mg/kg; 2 mg/kg for low dose; i.p.) 20 min before experiments. For chronic treatments, single daily i.p. injection of DCS (20 mg/kg) was administered for 7 days. For electrophysiology, DCS was dissolved in aCSF, and slices were bath incubated with DCS (20 μM) for at least 30 min before the start of experiments.

Data Acquisition Statistical Analysis

We performed our behavioral analysis in a double-blinded manner. All data were expressed as mean values with SEM. All statistical analyses were performed using GraphPad Prism software (version 7.0) (RRID: SCR_002798). Statistical significances were indicated in the figures as follows: *$p < 0.05$; **$p < 0.01$; ***$p < 0.001$; ns, not significant.

SUPPLEMENTAL INFORMATION

Supplemental Information includes Supplemental Experimental Procedures and seven figures and can be found with this article online at https://doi.org/10.1016/j.celrep.2018.05.087.

ACKNOWLEDGMENTS

We thank Sungsoo Kim at KAIST for helping with Golgi staining and Eunsil Cho at KIST (Korea Institute of Science and Technology) for helping with the graphical abstract design. This work was supported by the National Research Foundation of Korea (NRF) grant funded by the Korean government (NRF-2017R1A5A2015391 to Y.C.B.) and the Institute for Basic Science (IBS-R002-D1 to E.K.).

AUTHOR CONTRIBUTIONS

S.M.U., W.S., J.D.R., T.Y., and K.K. performed electrophysiology; S.H. performed immunoblot experiments; H.L. performed proximity ligation assays; J. Kim performed Sholl analysis; S.M.U., J. Kang, and Y.W.N. performed mouse breeding and behavioral experiments; S.M.U. performed immunohistochemistry; Y.S.C. performed electron microscopy; S.M.U. wrote the initial draft of the manuscript; Y.C.B. and E.K. supervised the projects and wrote the manuscript.

DECLARATION OF INTERESTS

The authors declare no competing interests.

Received: November 17, 2017
Revised: April 13, 2018
Accepted: May 25, 2018
Published: June 26, 2018

REFERENCES

Aoki-Suzuki, M., Yamada, K., Meerabux, J., Iwayama-Shigeno, Y., Ohba, H., Iwamoto, K., Takao, H., Toyota, T., Suto, Y., Nakatani, N., et al. (2005). A family-based association study and gene expression analyses of netrin-G1 and -G2 genes in schizophrenia. Biol. Psychiatry *57*, 382–393.

Bemben, M.A., Shipman, S.L., Nicoll, R.A., and Roche, K.W. (2015). The cellular and molecular landscape of neuroligins. Trends Neurosci. *38*, 496–505.

Bidinosti, M., Botta, P., Krüttner, S., Proenca, C.C., Stoehr, N., Bernhard, M., Fruh, I., Mueller, M., Bonenfant, D., Voshol, H., et al. (2016). CLK2 inhibition ameliorates autistic features associated with SHANK3 deficiency. Science *351*, 1199–1203.

Blundell, J., Blaiss, C.A., Etherton, M.R., Espinosa, F., Tabuchi, K., Walz, C., Bolliger, M.F., Südhof, T.C., and Powell, C.M. (2010). Neuroligin-1 deletion results in impaired spatial memory and increased repetitive behavior. J. Neurosci. *30*, 2115–2129.

Born, G., Grayton, H.M., Langhorst, H., Dudanova, I., Rohlmann, A., Woodward, B.W., Collier, D.A., Fernandes, C., and Missler, M. (2015). Genetic targeting of NRXN2 in mice unveils role in excitatory cortical synapse function and social behaviors. Front. Synaptic Neurosci. *7*, 3.

Bourgeron, T. (2015). From the genetic architecture to synaptic plasticity in autism spectrum disorder. Nat. Rev. Neurosci. *16*, 551–563.

Bozdagi, O., Tavassoli, T., and Buxbaum, J.D. (2013). Insulin-like growth factor-1 rescues synaptic and motor deficits in a mouse model of autism and developmental delay. Mol. Autism *4*, 9.

Brodkin, E.S., Hagemann, A., Nemetski, S.M., and Silver, L.M. (2004). Social approach-avoidance behavior of inbred mouse strains towards DBA/2 mice. Brain Res. *1002*, 151–157.

Burket, J.A., Benson, A.D., Tang, A.H., and Deutsch, S.I. (2013). D-Cycloserine improves sociability in the BTBR T+ Itpr3tf/J mouse model of autism spectrum disorders with altered Ras/Raf/ERK1/2 signaling. Brain Res. Bull. *96*, 62–70.

Burket, J.A., Benson, A.D., Green, T.L., Rook, J.M., Lindsley, C.W., Conn, P.J., and Deutsch, S.I. (2015a). Effects of VU0410120, a novel GlyT1 inhibitor, on measures of sociability, cognition and stereotypic behaviors in a

mouse model of autism. Prog. Neuropsychopharmacol. Biol. Psychiatry *61*, 10–17.

Burket, J.A., Benson, A.D., Tang, A.H., and Deutsch, S.I. (2015b). NMDA receptor activation regulates sociability by its effect on mTOR signaling activity. Prog. Neuropsychopharmacol. Biol. Psychiatry *60*, 60–65.

Chadman, K.K., Gong, S., Scattoni, M.L., Boltuck, S.E., Gandhy, S.U., Heintz, N., and Crawley, J.N. (2008). Minimal aberrant behavioral phenotypes of neuroligin-3 R451C knockin mice. Autism Res. *1*, 147–158.

Cheng, D., Hoogenraad, C.C., Rush, J., Ramm, E., Schlager, M.A., Duong, D.M., Xu, P., Wijayawardana, S.R., Hanfelt, J., Nakagawa, T., et al. (2006). Relative and absolute quantification of postsynaptic density proteome isolated from rat forebrain and cerebellum. Mol. Cell. Proteomics *5*, 1158–1170.

Connor, S.A., Ammendrup-Johnsen, I., Chan, A.W., Kishimoto, Y., Murayama, C., Kurihara, N., Tada, A., Ge, Y., Lu, H., Yan, R., et al. (2016). Altered cortical dynamics and cognitive function upon haploinsufficiency of the autism-linked excitatory synaptic suppressor MDGA2. Neuron *91*, 1052–1068.

Conzelman, G.M., Jr., and Jones, R.K. (1956). On the physiologic disposition of cycloserine in experimental animals. Am. Rev. Tuberc. *74*, 802–806.

Dachtler, J., Glasper, J., Cohen, R.N., Ivorra, J.L., Swiffen, D.J., Jackson, A.J., Harte, M.K., Rodgers, R.J., and Clapcote, S.J. (2014). Deletion of α-neurexin II results in autism-related behaviors in mice. Transl. Psychiatry *4*, e484.

de Wit, J., and Ghosh, A. (2014). Control of neural circuit formation by leucine-rich repeat proteins. Trends Neurosci. *37*, 539–550.

de Wit, J., and Ghosh, A. (2016). Specification of synaptic connectivity by cell surface interactions. Nat. Rev. Neurosci. *17*, 22–35.

DeNardo, L.A., de Wit, J., Otto-Hitt, S., and Ghosh, A. (2012). NGL-2 regulates input-specific synapse development in CA1 pyramidal neurons. Neuron *76*, 762–775.

Deutsch, S.I., Burket, J.A., Jacome, L.F., Cannon, W.R., and Herndon, A.L. (2011). D-Cycloserine improves the impaired sociability of the Balb/c mouse. Brain Res. Bull. *84*, 8–11.

Deutsch, S.I., Pepe, G.J., Burket, J.A., Winebarger, E.E., Herndon, A.L., and Benson, A.D. (2012). D-cycloserine improves sociability and spontaneous stereotypic behaviors in 4-week old mice. Brain Res. *1439*, 96–107.

Duffney, L.J., Wei, J., Cheng, J., Liu, W., Smith, K.R., Kittler, J.T., and Yan, Z. (2013). Shank3 deficiency induces NMDA receptor hypofunction via an actin-dependent mechanism. J. Neurosci. *33*, 15767–15778.

Duffney, L.J., Zhong, P., Wei, J., Matas, E., Cheng, J., Qin, L., Ma, K., Dietz, D.M., Kajiwara, Y., Buxbaum, J.D., and Yan, Z. (2015). Autism-like deficits in Shank3-deficient mice are rescued by targeting actin regulators. Cell Rep. *11*, 1400–1413.

Eastwood, S.L., and Harrison, P.J. (2008). Decreased mRNA expression of netrin-G1 and netrin-G2 in the temporal lobe in schizophrenia and bipolar disorder. Neuropsychopharmacology *33*, 933–945.

Etherton, M.R., Blaiss, C.A., Powell, C.M., and Südhof, T.C. (2009). Mouse neurexin-1alpha deletion causes correlated electrophysiological and behavioral changes consistent with cognitive impairments. Proc. Natl. Acad. Sci. USA *106*, 17998–18003.

Etherton, M., Földy, C., Sharma, M., Tabuchi, K., Liu, X., Shamloo, M., Malenka, R.C., and Südhof, T.C. (2011). Autism-linked neuroligin-3 R451C mutation differentially alters hippocampal and cortical synaptic function. Proc. Natl. Acad. Sci. USA *108*, 13764–13769.

Fitzjohn, S.M., Kingston, A.E., Lodge, D., and Collingridge, G.L. (1999). DHPG-induced LTD in area CA1 of juvenile rat hippocampus; characterisation and sensitivity to novel mGlu receptor antagonists. Neuropharmacology *38*, 1577–1583.

Fujita, E., Tanabe, Y., Shiota, A., Ueda, M., Suwa, K., Momoi, M.Y., and Momoi, T. (2008). Ultrasonic vocalization impairment of Foxp2 (R552H) knockin mice related to speech-language disorder and abnormality of Purkinje cells. Proc. Natl. Acad. Sci. USA *105*, 3117–3122.

Griebel, G., and Holmes, A. (2013). 50 years of hurdles and hope in anxiolytic drug discovery. Nat. Rev. Drug Discov. *12*, 667–687.

Holt, R., Barnby, G., Maestrini, E., Bacchelli, E., Brocklebank, D., Sousa, I., Mulder, E.J., Kantojärvi, K., Järvelä, I., Klauck, S.M., et al.; EU Autism MOLGEN Consortium (2010). Linkage and candidate gene studies of autism spectrum disorders in European populations. Eur. J. Hum. Genet. *18*, 1013–1019.

Huang, T.N., Chuang, H.C., Chou, W.H., Chen, C.Y., Wang, H.F., Chou, S.J., and Hsueh, Y.P. (2014). Tbr1 haploinsufficiency impairs amygdalar axonal projections and results in cognitive abnormality. Nat. Neurosci. *17*, 240–247.

Huber, K.M., Kayser, M.S., and Bear, M.F. (2000). Role for rapid dendritic protein synthesis in hippocampal mGluR-dependent long-term depression. Science *288*, 1254–1257.

Huber, K.M., Roder, J.C., and Bear, M.F. (2001). Chemical induction of mGluR5- and protein synthesis—dependent long-term depression in hippocampal area CA1. J. Neurophysiol. *86*, 321–325.

Iossifov, I., Ronemus, M., Levy, D., Wang, Z., Hakker, I., Rosenbaum, J., Yamrom, B., Lee, Y.H., Narzisi, G., Leotta, A., et al. (2012). De novo gene disruptions in children on the autistic spectrum. Neuron *74*, 285–299.

Jacobs, S., and Tsien, J.Z. (2017). Adult forebrain NMDA receptors gate social motivation and social memory. Neurobiol. Learn. Mem. *138*, 164–172.

Jacome, L.F., Burket, J.A., Herndon, A.L., and Deutsch, S.I. (2011). D-Cycloserine enhances social exploration in the Balb/c mouse. Brain Res. Bull. *85*, 141–144.

Jang, S., Lee, H., and Kim, E. (2017). Synaptic adhesion molecules and excitatory synaptic transmission. Curr. Opin. Neurobiol. *45*, 45–50.

Jaramillo, T.C., Speed, H.E., Xuan, Z., Reimers, J.M., Liu, S., and Powell, C.M. (2016). Altered striatal synaptic function and abnormal behaviour in Shank3 exon4-9 deletion mouse model of autism. Autism Res. *9*, 350–375.

Jentsch, J.D., and Roth, R.H. (1999). The neuropsychopharmacology of phencyclidine: from NMDA receptor hypofunction to the dopamine hypothesis of schizophrenia. Neuropsychopharmacology *20*, 201–225.

Jiang, Y.H., Yuen, R.K., Jin, X., Wang, M., Chen, N., Wu, X., Ju, J., Mei, J., Shi, Y., He, M., et al. (2013). Detection of clinically relevant genetic variants in autism spectrum disorder by whole-genome sequencing. Am. J. Hum. Genet. *93*, 249–263.

Kim, S., Burette, A., Chung, H.S., Kwon, S.K., Woo, J., Lee, H.W., Kim, K., Kim, H., Weinberg, R.J., and Kim, E. (2006). NGL family PSD-95-interacting adhesion molecules regulate excitatory synapse formation. Nat. Neurosci. *9*, 1294–1301.

Kirov, G., Pocklington, A.J., Holmans, P., Ivanov, D., Ikeda, M., Ruderfer, D., Moran, J., Chambert, K., Toncheva, D., Georgieva, L., et al. (2012). De novo CNV analysis implicates specific abnormalities of postsynaptic signalling complexes in the pathogenesis of schizophrenia. Mol. Psychiatry *17*, 142–153.

Ko, J., Choii, G., and Um, J.W. (2015). The balancing act of GABAergic synapse organizers. Trends Mol. Med. *21*, 256–268.

Kouser, M., Speed, H.E., Dewey, C.M., Reimers, J.M., Widman, A.J., Gupta, N., Liu, S., Jaramillo, T.C., Bangash, M., Xiao, B., et al. (2013). Loss of predominant Shank3 isoforms results in hippocampus-dependent impairments in behavior and synaptic transmission. J. Neurosci. *33*, 18448–18468.

Krueger, D.D., Tuffy, L.P., Papadopoulos, T., and Brose, N. (2012). The role of neurexins and neuroligins in the formation, maturation, and function of vertebrate synapses. Curr. Opin. Neurobiol. *22*, 412–422.

Lee, E.J., Choi, S.Y., and Kim, E. (2015a). NMDA receptor dysfunction in autism spectrum disorders. Curr. Opin. Pharmacol. *20*, 8–13.

Lee, E.J., Lee, H., Huang, T.N., Chung, C., Shin, W., Kim, K., Koh, J.Y., Hsueh, Y.P., and Kim, E. (2015b). Trans-synaptic zinc mobilization improves social interaction in two mouse models of autism through NMDAR activation. Nat. Commun. *6*, 7168.

Li, P., Xu, G., Li, G., and Wu, M. (2014). Function and mechanism of tumor suppressor gene LRRC4/NGL-2. Mol. Cancer *13*, 266.

Lin, J.C., Ho, W.H., Gurney, A., and Rosenthal, A. (2003). The netrin-G1 ligand NGL-1 promotes the outgrowth of thalamocortical axons. Nat. Neurosci. *6*, 1270–1276.

Lussier, M.P., Sanz-Clemente, A., and Roche, K.W. (2015). Dynamic regulation of N-methyl-d-aspartate (NMDA) and α-amino-3-hydroxy-5-methyl-4-isoxazolepropionic acid (AMPA) receptors by posttranslational modifications. J. Biol. Chem. *290*, 28596–28603.

Malkova, N.V., Yu, C.Z., Hsiao, E.Y., Moore, M.J., and Patterson, P.H. (2012). Maternal immune activation yields offspring displaying mouse versions of the three core symptoms of autism. Brain Behav. Immun. *26*, 607–616.

Matsukawa, H., Akiyoshi-Nishimura, S., Zhang, Q., Luján, R., Yamaguchi, K., Goto, H., Yaguchi, K., Hashikawa, T., Sano, C., Shigemoto, R., et al. (2014). Netrin-G/NGL complexes encode functional synaptic diversification. J. Neurosci. *34*, 15779–15792.

McAllister, K.H. (1994). D-cycloserine enhances social behaviour in individually-housed mice in the resident-intruder test. Psychopharmacology (Berl.) *116*, 317–325.

Missler, M., Südhof, T.C., and Biederer, T. (2012). Synaptic cell adhesion. Cold Spring Harb. Perspect. Biol. *4*, a005694.

Mohn, A.R., Gainetdinov, R.R., Caron, M.G., and Koller, B.H. (1999). Mice with reduced NMDA receptor expression display behaviors related to schizophrenia. Cell *98*, 427–436.

Nakashiba, T., Ikeda, T., Nishimura, S., Tashiro, K., Honjo, T., Culotti, J.G., and Itohara, S. (2000). Netrin-G1: a novel glycosyl phosphatidylinositol-linked mammalian netrin that is functionally divergent from classical netrins. J. Neurosci. *20*, 6540–6550.

Nakashiba, T., Nishimura, S., Ikeda, T., and Itohara, S. (2002). Complementary expression and neurite outgrowth activity of netrin-G subfamily members. Mech. Dev. *111*, 47–60.

Nishimura-Akiyoshi, S., Niimi, K., Nakashiba, T., and Itohara, S. (2007). Axonal netrin-Gs transneuronally determine lamina-specific subdendritic segments. Proc. Natl. Acad. Sci. USA *104*, 14801–14806.

Olney, J.W., Newcomer, J.W., and Farber, N.B. (1999). NMDA receptor hypofunction model of schizophrenia. J. Psychiatr. Res. *33*, 523–533.

Peng, J., Kim, M.J., Cheng, D., Duong, D.M., Gygi, S.P., and Sheng, M. (2004). Semiquantitative proteomic analysis of rat forebrain postsynaptic density fractions by mass spectrometry. J. Biol. Chem. *279*, 21003–21011.

Posey, D.J., Kem, D.L., Swiezy, N.B., Sweeten, T.L., Wiegand, R.E., and McDougle, C.J. (2004). A pilot study of D-cycloserine in subjects with autistic disorder. Am. J. Psychiatry *161*, 2115–2117.

Purcell, S.M., Moran, J.L., Fromer, M., Ruderfer, D., Solovieff, N., Roussos, P., O'Dushlaine, C., Chambert, K., Bergen, S.E., Kähler, A., et al. (2014). A polygenic burden of rare disruptive mutations in schizophrenia. Nature *506*, 185–190.

Qin, L., Ma, K., Wang, Z.J., Hu, Z., Matas, E., Wei, J., and Yan, Z. (2018). Social deficits in Shank3-deficient mouse models of autism are rescued by histone deacetylase (HDAC) inhibition. Nat. Neurosci. *21*, 564–575.

Rabaneda, L.G., Robles-Lanuza, E., Nieto-González, J.L., and Scholl, F.G. (2014). Neurexin dysfunction in adult neurons results in autistic-like behavior in mice. Cell Rep. *8*, 338–346.

Radyushkin, K., Hammerschmidt, K., Boretius, S., Varoqueaux, F., El-Kordi, A., Ronnenberg, A., Winter, D., Frahm, J., Fischer, J., Brose, N., and Ehrenreich, H. (2009). Neuroligin-3-deficient mice: model of a monogenic heritable form of autism with an olfactory deficit. Genes Brain Behav. *8*, 416–425.

Reissner, C., Runkel, F., and Missler, M. (2013). Neurexins. Genome Biol. *14*, 213.

Rippberger, H., van Gaalen, M.M., Schwarting, R.K., and Wohr, M. (2015). Environmental and pharmacological modulation of amphetamine-induced 50-kHz ultrasonic vocalizations in rats. Curr. Neuropharmacol. *13*, 220–232.

Rodgers, R.J., Harvest, H., Hassall, C., and Kaddour, L.A. (2011). D-cycloserine enhances memory consolidation in the plus-maze retest paradigm. Behav. Neurosci. *125*, 106–116.

Rothwell, P.E., Fuccillo, M.V., Maxeiner, S., Hayton, S.J., Gokce, O., Lim, B.K., Fowler, S.C., Malenka, R.C., and Südhof, T.C. (2014). Autism-associated neuroligin-3 mutations commonly impair striatal circuits to boost repetitive behaviors. Cell *158*, 198–212.

Sangu, N., Shimojima, K., Takahashi, Y., Ohashi, T., Tohyama, J., and Yamamoto, T. (2017). A 7q31.33q32.1 microdeletion including *LRRC4* and *GRM8* is associated with severe intellectual disability and characteristics of autism. Hum. Genome Var. *4*, 17001.

Sankoorikal, G.M., Kaercher, K.A., Boon, C.J., Lee, J.K., and Brodkin, E.S. (2006). A mouse model system for genetic analysis of sociability: C57BL/6J versus BALB/cJ inbred mouse strains. Biol. Psychiatry *59*, 415–423.

Scattoni, M.L., Gandhy, S.U., Ricceri, L., and Crawley, J.N. (2008). Unusual repertoire of vocalizations in the BTBR T+tf/J mouse model of autism. PLoS ONE *3*, e3067.

Scattoni, M.L., Crawley, J., and Ricceri, L. (2009). Ultrasonic vocalizations: a tool for behavioural phenotyping of mouse models of neurodevelopmental disorders. Neurosci. Biobehav. Rev. *33*, 508–515.

Shen, K., and Scheiffele, P. (2010). Genetics and cell biology of building specific synaptic connectivity. Annu. Rev. Neurosci. *33*, 473–507.

Soto, F., Watkins, K.L., Johnson, R.E., Schottler, F., and Kerschensteiner, D. (2013). NGL-2 regulates pathway-specific neurite growth and lamination, synapse formation, and signal transmission in the retina. J. Neurosci. *33*, 11949–11959.

Soto, F., Zhao, L., and Kerschensteiner, D. (2018). Synapse maintenance and restoration in the retina by NGL2. eLife *7*, e30388.

Südhof, T.C. (2017). Synaptic neurexin complexes: a molecular code for the logic of neural circuits. Cell *171*, 745–769.

Sugimoto, H., Okabe, S., Kato, M., Koshida, N., Shiroishi, T., Mogi, K., Kikusui, T., and Koide, T. (2011). A role for strain differences in waveforms of ultrasonic vocalizations during male-female interaction. PLoS ONE *6*, e22093.

Tabuchi, K., Blundell, J., Etherton, M.R., Hammer, R.E., Liu, X., Powell, C.M., and Südhof, T.C. (2007). A neuroligin-3 mutation implicated in autism increases inhibitory synaptic transmission in mice. Science *318*, 71–76.

Takahashi, H., and Craig, A.M. (2013). Protein tyrosine phosphatases PTPδ, PTPσ, and LAR: presynaptic hubs for synapse organization. Trends Neurosci. *36*, 522–534.

Um, J.W., and Ko, J. (2013). LAR-RPTPs: synaptic adhesion molecules that shape synapse development. Trends Cell Biol. *23*, 465–475.

Urbano, M., Okwara, L., Manser, P., Hartmann, K., Herndon, A., and Deutsch, S.I. (2014). A trial of D-cycloserine to treat stereotypies in older adolescents and young adults with autism spectrum disorder. Clin. Neuropharmacol. *37*, 69–72.

Valnegri, P., Sala, C., and Passafaro, M. (2012). Synaptic dysfunction and intellectual disability. Adv. Exp. Med. Biol. *970*, 433–449.

Wang, H., Liang, S., Burgdorf, J., Wess, J., and Yeomans, J. (2008). Ultrasonic vocalizations induced by sex and amphetamine in M2, M4, M5 muscarinic and D2 dopamine receptor knockout mice. PLoS ONE *3*, e1893.

Wang, X., McCoy, P.A., Rodriguiz, R.M., Pan, Y., Je, H.S., Roberts, A.C., Kim, C.J., Berrios, J., Colvin, J.S., Bousquet-Moore, D., et al. (2011). Synaptic dysfunction and abnormal behaviors in mice lacking major isoforms of Shank3. Hum. Mol. Genet. *20*, 3093–3108.

Won, H., Lee, H.R., Gee, H.Y., Mah, W., Kim, J.I., Lee, J., Ha, S., Chung, C., Jung, E.S., Cho, Y.S., et al. (2012). Autistic-like social behaviour in Shank2-mutant mice improved by restoring NMDA receptor function. Nature *486*, 261–265.

Woo, J., Kwon, S.K., Choi, S., Kim, S., Lee, J.R., Dunah, A.W., Sheng, M., and Kim, E. (2009a). Trans-synaptic adhesion between NGL-3 and LAR regulates the formation of excitatory synapses. Nat. Neurosci. *12*, 428–437.

Woo, J., Kwon, S.K., and Kim, E. (2009b). The NGL family of leucine-rich repeat-containing synaptic adhesion molecules. Mol. Cell. Neurosci. *42*, 1–10.

Yin, Y., Miner, J.H., and Sanes, J.R. (2002). Laminets: laminin- and netrin-related genes expressed in distinct neuronal subsets. Mol. Cell. Neurosci. *19*, 344–358.

Young, J.W., Powell, S.B., Risbrough, V., Marston, H.M., and Geyer, M.A. (2009). Using the MATRICS to guide development of a preclinical cognitive test battery for research in schizophrenia. Pharmacol. Ther. *122*, 150–202.

Yuzaki, M. (2011). Cbln1 and its family proteins in synapse formation and maintenance. Curr. Opin. Neurobiol. *21*, 215–220.

Zhang, W., Rajan, I., Savelieva, K.V., Wang, C.Y., Vogel, P., Kelly, M., Xu, N., Hasson, B., Jarman, W., and Lanthorn, T.H. (2008). Netrin-G2 and netrin-G2 ligand are both required for normal auditory responsiveness. Genes Brain Behav. *7*, 385–392.